BRAIN STIMULATION

Chronic embedded cortico-thalamic closed-loop deep brain stimulation for the treatment of essential tremor

Enrico Opri[1]*, Stephanie Cernera[1], Rene Molina[2], Robert S. Eisinger[3], Jackson N. Cagle[1], Leonardo Almeida[3], Timothy Denison[4], Michael S. Okun[3], Kelly D. Foote[3†], Aysegul Gunduz[1,2,3†]

Deep brain stimulation (DBS) is an approved therapy for the treatment of medically refractory and severe movement disorders. However, most existing neurostimulators can only apply continuous stimulation [open-loop DBS (OL-DBS)], ignoring patient behavior and environmental factors, which consequently leads to an inefficient therapy, thus limiting the therapeutic window. Here, we established the feasibility of a self-adjusting therapeutic DBS [closed-loop DBS (CL-DBS)], fully embedded in a chronic investigational neurostimulator (Activa PC + S), for three patients affected by essential tremor (ET) enrolled in a longitudinal (6 months) within-subject crossover protocol (DBS OFF, OL-DBS, and CL-DBS). Most patients with ET experience involuntary limb tremor during goal-directed movements, but not during rest. Hence, the proposed CL-DBS paradigm explored the efficacy of modulating the stimulation amplitude based on patient-specific motor behavior, suppressing the pathological tremor on-demand based on a cortical electrode detecting upper limb motor activity. Here, we demonstrated how the proposed stimulation paradigm was able to achieve clinical efficacy and tremor suppression comparable with OL-DBS in a range of movements (cup reaching, proximal and distal posture, water pouring, and writing) while having a consistent reduction in energy delivery. The proposed paradigm is an important step toward a behaviorally modulated fully embedded DBS system, capable of delivering stimulation only when needed, and potentially mitigating pitfalls of OL-DBS, such as DBS-induced side effects and premature device replacement.

INTRODUCTION

Current commercially available deep brain stimulation (DBS) devices effectively suppress debilitating tremor in movement disorders such as essential tremor (ET) and Parkinson's disease. Yet, current stimulation approaches (continuous stimulation, also known as open-loop stimulation) lack integration with patient behavior and environmental factors. Such lack of flexibility leads to unnecessary, constant stimulation and is likely associated with a higher incidence of DBS-related side effects, such as impaired proprioception, gait issues, or speech dysfunction (*1*–*5*). In addition, current literature has revealed that current open-loop paradigms may contribute to stimulation tolerance (*6*, *7*). In the absence of tremor, ongoing continuous DBS delivery translates to a wasteful energy management and consequently to an excessive incidence of battery replacement surgeries. Furthermore, current standard of care requires labor-intensive adjustment of stimulation parameters to achieve the desired magnitude of tremor reduction while minimizing side effects. If this result cannot be achieved with one parameter setting, a patient may have to actively switch between a configuration optimized for maximal tremor suppression and a less aggressive one with modest tremor suppression but with fewer side effects. For example, patients may choose the first configuration for writing or eating because it results in minimal tremor, and switch to the latter when speaking to reduce the stimulation-induced speech dysfunction. Thus, there is a critical need for advances in DBS technology with a focus on decoupling both the patient and clinician from continuous adjustments. Therefore, our work aims to deliver a "set and forget" approach to DBS, which independently self-adjusts based on real-time tracking of motor behavior.

In this study, we focused on ET, which is among the most common movement disorders and the most prevalent tremor disorder (*8*). ET is a progressive, degenerative brain disorder that results in increasingly debilitating tremor and afflicts an estimated 7 million people in the United States (2.2% of the population) (*9*) and from 0.4 to 6.3% of people worldwide (*10*). ET is directly linked to progressive functional impairment (*11*, *12*), social embarrassment (*12*, *13*), and even depression (*14*). ET is defined as a bilateral, rhythmical, involuntary oscillatory (~4 to 12 Hz) movement of the upper limbs (*15*). The subjects in our study were disabled by the intention tremor subtype of ET, which typically occurs in the hands and arms during the initiation and execution of goal-directed reaching motions, while it is absent or non-disabling at rest (*16*, *17*). Despite the numerous therapeutic modalities available (*18*), the effectiveness of non-surgical treatment options (medications, botox, and assistive devices) in moderate to severe tremor has been disappointing (*19*–*21*). In addition, 65% of those suffering from upper limb tremor report serious difficulties during their daily lives (*22*). For patients with medically refractory and severe tremor, DBS has been widely adopted as a treatment option. A pathological synchronous oscillation in a neuronal network involving mainly the ventralis intermediate nucleus (VIM) of the thalamus, the premotor (PM), the primary motor (M1) cortices, and the cerebellum has been suggested (*23*, *24*). Hence, the most common target for ET DBS therapy is the VIM thalamus (*25*).

This work introduces a chronically implanted and fully embedded closed-loop DBS (CL-DBS) paradigm for patients affected by ET, tailoring the device to suppress the pathological phenotype of interest (tremor) only when present. We used Activa PC + S bidirectional neurostimulators (Medtronic) that allow chronic recordings (*26*, *27*)

[1]J. Crayton Pruitt Family Department of Biomedical Engineering, University of Florida, Gainesville, FL 32611, USA. [2]Electrical and Computer Engineering, University of Florida, Gainesville, FL 32603, USA. [3]Norman Fixel Institute for Neurological Diseases at UF Health, Departments of Neurology and Neurosurgery, University of Florida, Gainesville, FL 32608, USA. [4]Department of Engineering Science, University of Oxford, Oxford OX1 3PJ, UK.
*Corresponding author. Email: enrico.opri@ufl.edu
†This paper was a product of the NIH BRAIN Initiative, and multiple principal investigators A.G. and K.D.F. serve as co-senior authors.

and prototyping of closed-loop therapies. We focused on detecting movement onset (MO)/termination for stimulation delivery on-demand. This was possible because the tremor always manifested with movement. We considered that MO preceded tremor presentation, and we therefore planned to deliver stimulation as rapidly as possible using detection of MO/termination through a subdural electrode array placed over the hand motor area. Together with a bidirectional neurostimulator connected to a standard DBS electrode array in the VIM, it enabled cortically driven on-demand thalamic stimulation.

RESULTS

Device implantation and offline feasibility

To evaluate the feasibility of closed-loop in patients affected by ET, we implanted the Activa PC + S neurostimulators in three subjects affected by ET (table S1) and evaluated the embedded control algorithm performances longitudinally (6 months). We designed an algorithm to drive stimulation with detection of movement execution, using low-frequency oscillations (LFOs) recorded from unilateral subdural cortical electrodes. The cortical target was the M1 hand motor region ipsilateral to the VIM lead, both contralateral to the most affected hand. Details of the cortical electrode positioning are shown in Fig. 1, A to C, for subjects ET01, ET02, and ET03, respectively. Thalamic DBS leads positions are shown in Fig. 1D normalized to an Montreal Neurological Institute (MNI) brain, together with structures of interest. The system was implemented by first training the algorithm parameters offline with data streamed using a telemetry wand (Nexus-D) (*28*) (setup described in Fig. 2A), collected during a cued arm movement task (both left and right arms) (task timeline is shown in Fig. 2B, and single data collection and related training are shown in Fig. 2, C and D). Next, it was tested online with the embedded classifier within Activa PC + S (*26*, *27*). This prototyping strategy is described in Supplementary Materials and Methods and in previous work (*28*, *29*). In addition to user-driven algorithm requirements, we also implemented risk mitigations for the closed-loop design to limit the impact of potential hazards [see the "Risk and mitigations" section in Materials and Methods; (*30*)]. The subjects were left on the continuous conventional DBS [open-loop DBS (OL-DBS)] settings between monthly visits during this feasibility study. Each month, for 6 months, OL-DBS settings were compared to CL-DBS settings in-clinic. The closed-loop settings were chosen with equal or decreased parameters (such as decreasing amplitude, stimulation frequency, and pulse width) to avoid any off-target stimulation side effects, such as paresthesia during stimulation onset (SO). The preferred parameter reduction involved the pulse width, which has the benefit of reducing current spread and reducing stimulation-induced paresthesia (*31*, *32*). Patient tolerance to closed-loop stimulation was chosen as a hard constraint (go/no-go milestone), considering that, for closed-loop stimulation to be a viable therapeutic option, patient comfort had to be as important as tremor suppression. The data collected postoperatively demonstrated the possibility of achieving single-trial detection of movement execution, during cued (task timeline in Fig. 3A) and volitional movement trials, using contacts over M1 and VIM (Fig. 3, B to D). Similarly to previous work involving patients affected by ET (*33*), there was a clear power deviation during movement in the cortical M1 activity (decrease in LFO, increase in high broadband activity above 60 Hz) [Fig. 3, B (top spectrogram) and C (left)]. The power deviation during movement in the VIM activity (decrease in LFO) [Fig. 3, B (bottom spectrogram) and C (right)] could have been sufficient to achieve movement detection without

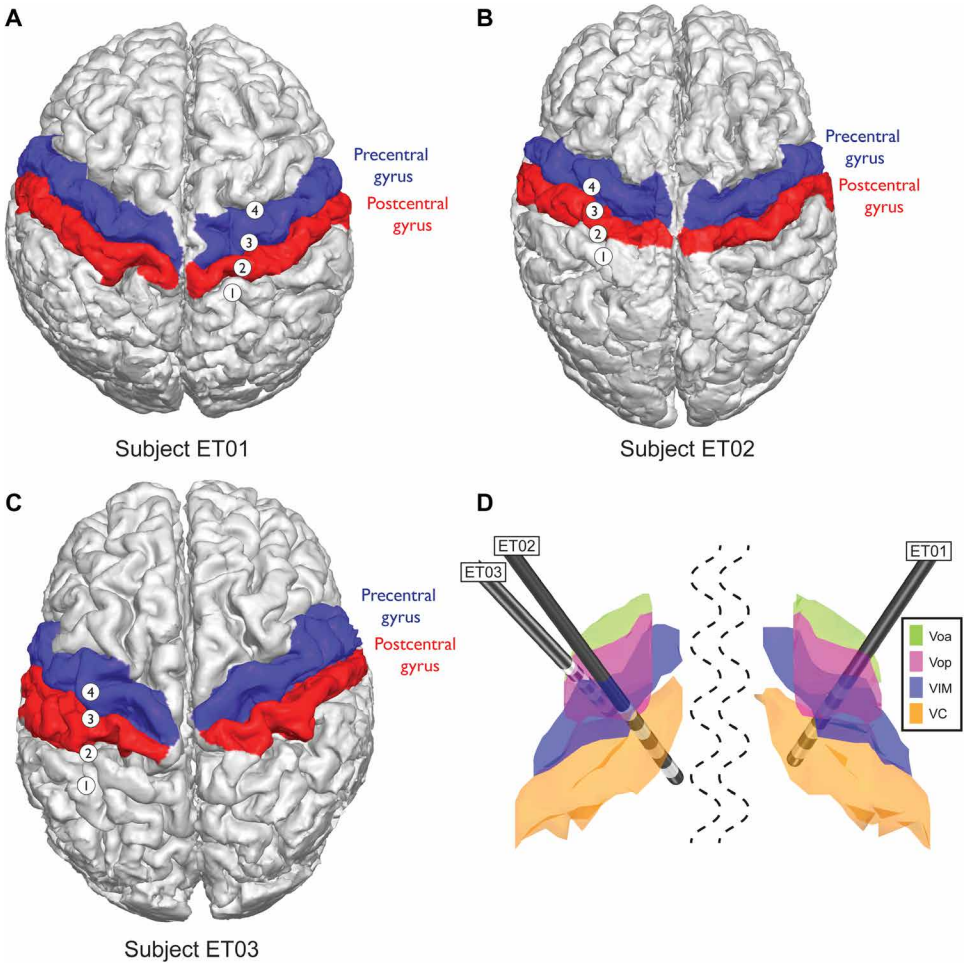

Fig. 1. Patient-specific magnetic resonance imaging–computed tomography reconstruction and segmentation of cortical and thalamic regions in ET closed-loop patients. (**A**) Subject ET01, (**B**) subject ET02, and (**C**) subject ET03 cortical segmentations. Red, postcentral gyrus; blue, precentral gyrus, known as primary motor cortex (M1). (**D**) Subcortical thalamic segmentation with overlaid DBS lead positioning based on surgical planning and all normalized to an MNI brain. The structures shown are ventralis oralis anterior (Voa; green), ventralis oralis posterior (Vop; magenta), ventralis intermediate nucleus (VIM; blue), and nucleus ventralis caudalis (VC; orange).

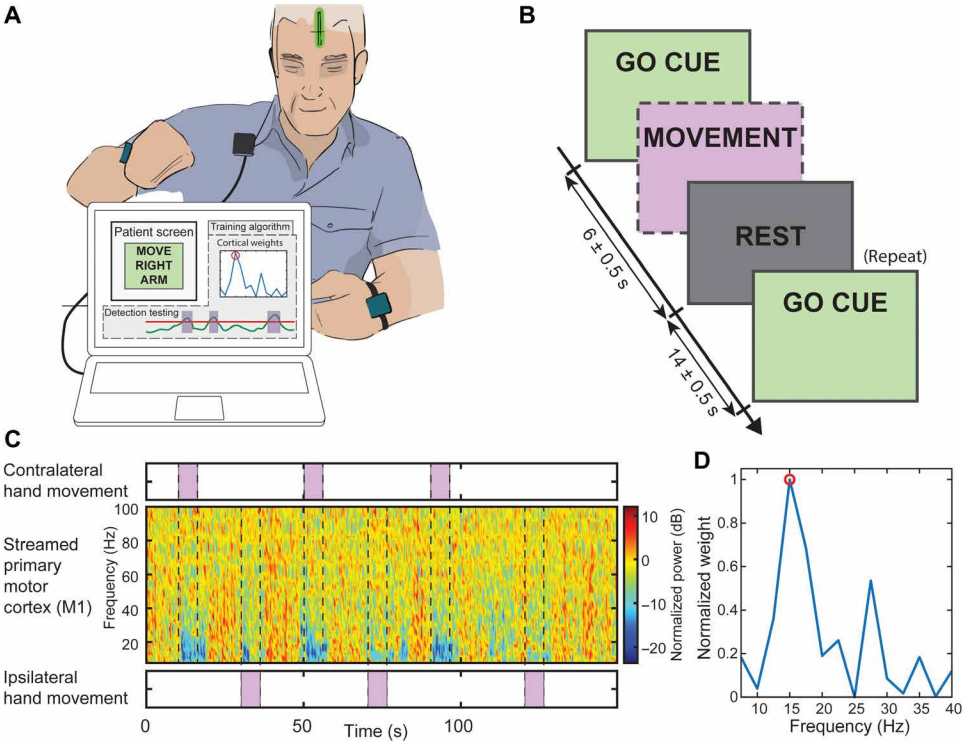

Fig. 2. Training session for onboard movement detection. (**A**) Setup for the training of the onboard weights used by the embedded LDA to actuate the stimulation. The patient is prompted to move (visual GO CUE) while data are being streamed through Nexus-D telemetry wand from the cortical strip (shown as a green strip in the patient head) to an external computer (the training algorithm output is not shown to the patient). (**B**) Task timeline of the recordings. The boxes with a dashed border indicate the un-cued actions that the subject took during the task. The patient was cued (GO CUE) to execute arm movement (with left or right arm) until the REST cue was delivered. The task was repeated interleaving the hands used in a randomized pattern. (**C**) Spectrogram collected from M1 through the telemetry wand, aligned with the executed cued movement (contralateral and ipsilateral). The spectrogram was used as features for a Fisher score feature selection algorithm, for which the output is shown in (**D**). One or two features were selected, and the Activa PC + S neurostimulator was set up accordingly. After identifying the features of interest, the same paradigm was repeated to obtain the weights and threshold for the stimulation delivery based on power features.

relying on the cortical M1 activity; however, it was not a viable option because the stimulation overwhelmed the amplifier stage for the VIM channel, leading to unrecoverable brain activity from contacts adjacent to the stimulating contact within the same DBS lead (saturated VIM channel shown in fig. S1). However, even during stimulation, it was possible to recover viable spectral changes from the cortical contacts during a cued movement task (fig. S2). To be able to minimize stimulation artifacts, we based the closed-loop implementation only on the M1 contacts and a VIM bipolar stimulation paradigm, because monopolar stimulation resulted in excessive contamination of M1 power estimates.

Longitudinal clinical efficacy of CL-DBS compared with OL-DBS

Clinical outcomes were evaluated at each monthly visit for 6 months, for each of the DBS settings: DBS OFF, OL-DBS, and CL-DBS. The settings used during each month are reported in table S2. Clinical efficacy was determined using the Fahn-Tolosa-Marin Tremor Rating Scale (TRS) (*34*, *35*), where the best outcome was associated with the lowest score. For the evaluation of the effectiveness of the DBS programming, only part A (assesses examiner-reported tremor location/severity) and part B (assesses examiner-reported functional disability related to tremor) were taken into consideration. Parts A and B of the TRS assessment include testing for water pouring, writing, spiral and line drawing, finger to nose, proximal and distal posture of the upper limbs, standing, and face/neck tremor. Video recordings were collected during the administration of the TRS and rated by a blinded neurologist. The operators configuring the stimulation could not be blinded because of the complexity of the setup; however, they were not involved in clinical scoring. The patient may have not been completely blinded regarding the DBS setting in use based on the incidence of paresthesia. Few OL-DBS settings, such as monopolar stimulation that was a common setting in the initial months (table S2), caused temporary paresthesia when activated, resolving under 1 min. The optimized CL-DBS settings used during TRS evaluation did not cause paresthesia and consequently were not distinguishable from the DBS OFF settings and the late OL-DBS settings. The overall scores for the total body TRS revealed (Fig. 4A) a clear score decrease (improvement) of OL-DBS [mixed-model analysis of variance (ANOVA) with patient as random effect: total TRS: $F_{1,31} = 38.182$, $P = 7.377 \times 10^{-7}$; contralateral side TRS: $F_{1,31} = 32.476$, $P = 2.898 \times 10^{-6}$] and CL-DBS (mixed-model ANOVA with patient as random effect: total TRS: $F_{1,24} = 20.645$, $P = 0.00013$; contralateral side TRS: $F_{1,24} = 18.529$, $P = 0.00024$) compared to DBS OFF for all three patients. The percent decrease from DBS OFF was −33.8% (SD = 17.8%) for total TRS [for contralateral side, TRS was −52.7% (SD = 26.9%)] with OL-DBS, whereas with CL-DBS was −32.7% (SD = 12.7%) for total TRS [for contralateral side TRS, there was a −47.4% (SD = 14.3%) decrease]. OL-DBS TRS score did not show statistical difference from CL-DBS (total TRS: $t_7 = 0.000$, $P = 1.000$; contralateral only TRS: $t_7 = -0.6070$, $P = 0.5630$). A two one-sided *t* test (TOST) procedure showed equivalence in clinical efficacy for OL-DBS and CL-DBS within a 2 TRS point interval (total TRS lower equivalence bound: $t_7 = 4.7329$, $P = 0.0011$; upper equivalence bound: $t_7 = -4.7329$, $P = 0.0011$; contralateral side TRS lower equivalence bound: $t_7 = 4.2488$, $P = 0.0019$; upper equivalence bound: $t_7 = -5.4628$, $P = 0.0005$). The 2 TRS point interval was chosen considering one point of uncertainty for each TRS test in the comparison (one for OL-DBS and one for CL-DBS), which corresponds to 1.72% of the maximum score possible (116 points for the total TRS and 5% of the maximum score possible 40 for the contralateral side TRS).

Sensor-based tremor quantification during CL-DBS compared with OL-DBS

In addition, we report tremor amplitude changes during both therapies using accelerometry data (Fig. 4B), as described in previous work (*36*, *37*). Consistent with TRS scores (Fig. 4A), the accelerometry of

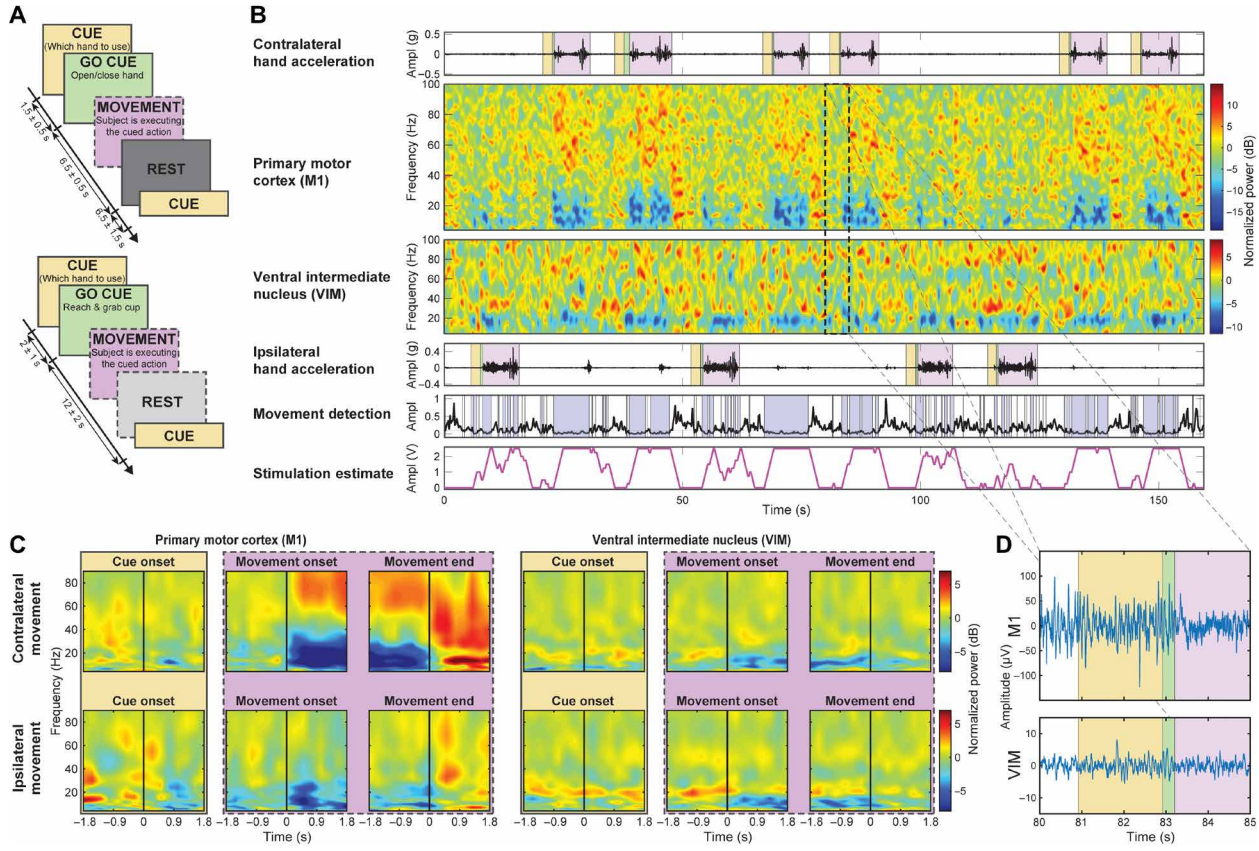

Fig. 3. Task timeline and raw and spectral analyses with detection test bench. (**A**) Task timeline of the recordings. Top: Cued-go hand opening and closing task. Bottom: Cued-go cup reaching task, where no rest cues were delivered. The boxes with a dashed border indicate the volitional actions the subject took during the task (following previous cued commands). (**B**) Data collected in a single patient (ET03) during a single cued-go cup reaching task along with contralateral and ipsilateral hand accelerations with respect to the side of implantation. The subjects were asked to prepare to move with the CUED hand (yellow). GO CUE (green) represents when the subjects were asked to reach the cup, and MOVEMENT (violet) represents when the patients proceeded to execute the movement. The bottom two plots show the outcome of the embedded movement detection (blue blocks indicate movement detection) and the stimulation estimate (considering the delivering during the contralateral/affected limb, it had an accuracy of 96.44%, a specificity of 95%, and a sensitivity of 97%). No DBS was delivered during this trial. Stimulation estimate is solely presented to show the feasibility of the paradigm (stimulation range = 0 to 2.5 V, ramp-up/down = 1.25 V/s). Therefore, tremor was present during each movement, unsuppressed. (**C**) Normalized event-related desynchronization and synchronization (ERD-ERS) spectrograms aligned to three events: cue, MO, and movement termination (MT) for contralateral and ipsilateral hand movements. (**D**) Zoomed section of raw recording from (B) during contralateral reaching movement.

the affected limb (limb contralateral to the DBS lead) showed a clear decrease (improvement) of OL-DBS (mixed-model ANOVA with patient as random effect, $F_{1,29} = 8.9479$, $P = 0.0056$) and CL-DBS (mixed-model ANOVA with patient as random effect, $F_{1,23} = 6.1502$, $P = 0.0209$) compared to DBS OFF for all three patients. The tremor amplitude percent decrease from DBS OFF was −42.8% (SD = 23.6%) with OL-DBS, whereas with CL-DBS was −44.4% (SD = 16.3%). OL-DBS tremor amplitude did not show statistical difference from CL-DBS tremor amplitude ($t_7 = 1.1276$, $P = 0.297$). TOST procedure showed equivalence in tremor amplitude for OL-DBS − CL-DBS within a 0.1 m/s^2 point interval (lower equivalence bound: $t_7 = 4.1061$, $P = 0.0023$; upper equivalence bound: $t_7 = -2.3433$, $P = 0.0258$). The 0.1 point TRS interval was chosen considering estimation uncertainty and the minimum sensible difference for tremor severity considerations (*37*). We further segmented the movement and stimulation delivery in subintervals marked by event of interest, such as the SO, the time when the stimulation reached its maximum amplitude [maximum stimulation amplitude reached (MSAR)], and the MO (described in Fig. 4C). We then focused our interest on the tremor amplitude from MO to MSAR (interval MO-MSAR) and from MSAR to movement termination (interval MSAR-MT). Considering that DBS OFF and OL-DBS settings do not have a ramp-up interval, for comparison across the different DBS settings (DBS OFF, OL-DBS, and CL-DBS), we used the MO-MSAR interval from the CL-DBS executed during the same month. If no CL-DBS was recorded during that month, we used the patient-matched MO-MSAR average. Similar to what is shown for the tremor amplitude during the whole movement period, during the MSAR-MT interval, there was a clear decrease (improvement) of OL-DBS (mixed-model ANOVA with patient as random effect: $F_{1,29} = 7.4617$, $P = 0.0106$) and CL-DBS (mixed-model ANOVA with patient as random effect: $F_{1,23} = 5.6956$, $P = 0.0256$) compared to DBS OFF for all three patients (Fig. 4D, bottom). The tremor amplitude percent decrease from DBS OFF was −39.0% (SD = 28.4%) for OL-DBS, whereas for CL-DBS was −39.9% (SD = 26.5%). However, during the MO-MSAR interval, the tremor amplitude had a more modest decrease from DBS OFF (Fig. 4D, top), with −17.5% (SD = 36.9%) for OL-DBS (mixed-model ANOVA with patients as random effect: $F_{1,29} = 1.4196$, $P = 0.2431$), whereas for CL-DBS was −19.6% (SD = 24.9%) (mixed-model ANOVA with patients as random effect: $F_{1,23} = 1.9517$, $P = 0.1757$). Neither

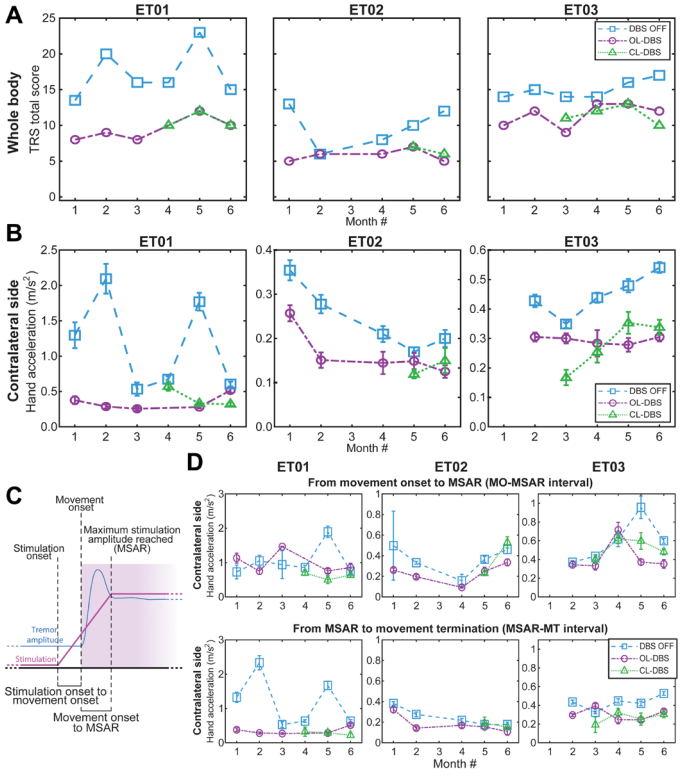

Fig. 4. Longitudinal clinical outcomes for CL-DBS during specific stimulation and movement events. (**A**) Clinical TRS over 6-month visits across different DBS modalities. CL-DBS scores are presented starting with the month it was established in each patient. For patient ET01, the score for OL-DBS is missing on month 4 due to subject exhaustion. For patient ET02, month 3 scores were not assessed due to medical reasons unrelated to the study. (**B**) Tremor amplitude based on acceleration during the execution of the TRS clinical assessment shown in (A). For patient ET03, month 1 inertial data during TRS evaluation were not collected. (**C**) Diagram of the subdivisions of interest: SO, MO, time maximum stimulation amplitude reached (MSAR), MT, delay MO to SO (interval MO-SO), and delay MO to MSAR (interval MO-MSAR). (**D**) Tremor amplitude based on acceleration during the execution of the TRS clinical assessment over 6 monthly visits across different DBS modalities, as shown in (A) and (B). Top, tremor amplitude during the MO-SO interval; bottom, tremor amplitude during the MSAR-MT interval. For patient ET01, the score for OL-DBS is missing on month 4 due to subject exhaustion. For patient ET02, month 3 scores were not assessed due to medical reasons unrelated to the study. For patient ET03 month, inertial data during TRS evaluation were not collected. DBS OFF and OL-DBS settings do not have a ramp-up interval, and to achieve a comparison across different DBS settings (DBS OFF, OL-DBS, and CL-DBS), we use the MO-MSAR interval from the CL-DBS recorded during the same month. If no CL-DBS was executed during that month, we used the patient-matched MO-MSAR average.

of the DBS settings (OL-DBS and CL-DBS) led to differences from DBS OFF during the MO-MSAR interval, leading to the consideration that there is a brief leftover tremor at every initial movement regardless of the stimulation paradigm.

Longitudinal performance of the fully embedded CL-DBS paradigm

The performance of the closed-loop algorithm was evaluated in the fully embedded system by comparing the stimulation delivery with most tremor-affected arm movement (contralateral limb to the implant, based on acceleration traces) and obtaining accuracy, sensitivity, and specificity measures. Figure 5 demonstrates the implementation of the closed-loop paradigm in a single subject in a volitional reaching task (ET01, third month), in which the patient simulated a typical upper extremity movement consisting of reaching and bringing a cup toward themselves. The power in the LFO range was used to detect MO and termination (for this recording were set with 15 and 25 Hz as center frequency and 5 Hz of bandwidth each), actuating the stimulation delivery (Fig. 5, bottom row). Stimulation did not impede the detection of MO and end, because the artifact leakage did not affect the spectral band of interest (LFO) in M1 (fig. S3). During the volitional cup reaching task, the detection performance in all patients across months showed high accuracy [92.55% (SD = 5.23%)], sensitivity [94.17% (SD = 8.28%)], specificity [90.99% (SD = 5.26%)], and precision [90.61% (SD = 7.41%)]. The longitudinal patient-specific performance is given in Fig. 6A and fig. S4, the average patient-specific performance is given in Fig. 6B, and the overall performance across patients is given in Fig. 6C. A single-task comparison of the therapeutic performance between DBS OFF, CL-DBS, and OL-DBS is shown for each patient (movie S1: ET01 executing a volitional cup reaching task; movie S2: ET02 executing a cued-go cup reaching task; movie S3: ET03 executing a volitional cup reaching task). Electromyography (EMG) and inertial sensors were used only for labeling and tremor evaluations, not as inputs for the control algorithm. Furthermore, the interval MO-SO showed different performances in how early the detector triggered stimulation with respect to MO (Fig. 6D), with an average delay of −0.23 s (SD = 1.21 s) across patients. Specifically, for each patient, the MO-SO was as follows: ET01, −0.76 s (SD = 1.38 s); ET02, −0.22 s (SD = 1.25 s); ET03, 0.26 s (SD = 0.79 s). The interval MO-MSAR is further dependent on the ramp-up time of stimulation [maximum amplitude (V) divided by ramp-up (V/s)] set for each patient at each month, leading to an average delay from MO to MSAR of 1.72 (SD = 1.15 s) across patients [ET01, 1.13 s (SD = 1.36 s); ET02, 2.08 s (SD = 1.13 s); ET03, 1.95 s (SD = 0.70 s)].

Energy savings of CL-DBS

We evaluated the energy savings for the proposed closed-loop stimulation paradigm during both in-clinic testing and at home (between two consecutive daily clinic visits, from the afternoon to the morning of the next day), during a typical daily real-life usage (labeled as short-term daily usage). The total electrical energy delivered (TEED) (*38*) was computed for both OL-DBS and CL-DBS conditions. TEEDs are normalized to the duration of the task to avoid bias due to each task length (see the "Classification performance and energy consumption" section in Supplementary Materials and Methods). The energy saving is obtained by comparing the TEED for CL-DBS with the maximum TEED possible with CL-DBS settings (considering CL-DBS always in detect state, leading to CL-DBS being always at the maximum stimulation amplitude possible). The maximum TEED for CL-DBS is equivalent to the TEED of an open-loop paradigm, which uses the same DBS parameters of CL-DBS. The mean energy saving for CL-DBS was 57.98% (SD = 14.12%) during the clinic testing (Fig. 6E, left) and 50.15% (SD = 11.47%) while at home (Fig. 6E, right). Taking into consideration both clinical effectiveness and energy savings, the results revealed equal clinical benefit for less energy consumption (Fig. 6F), as shown by the TEED (considered as percent difference from the same month OL-DBS TEED), with mixed-model ANOVA revealing a main effect of DBS type (OL-DBS versus CL-DBS) ($F_{1,21} = 39.63$, $P = 0.000003$) but not for TRS ($F_{1,21} = 3.224 \times 10^{-29}$, $P = 1.000$) (figs. S5 and 6F). Post

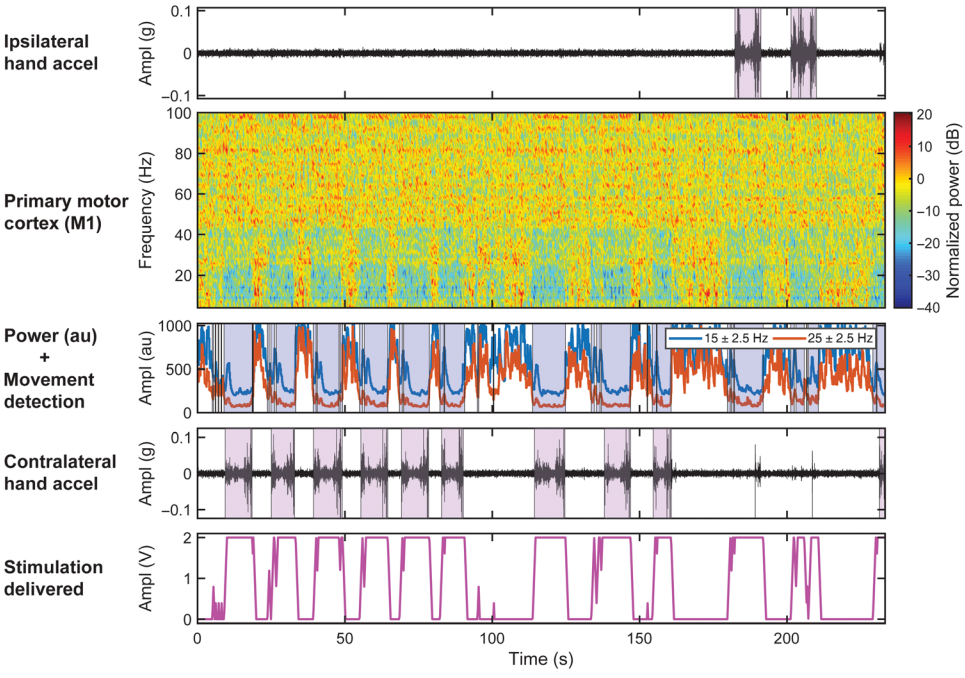

Fig. 5. Implementation of CL-DBS in patient affected by ET (ET01, third month). Brain activity was recorded during a volitional reaching task with simulated drinking (patients reached for the cup, brought it close to their mouths, and put it back) along with ipsilateral and contralateral hand accelerometer traces. The violet boxes represent the movement initiation toward the target (cup). The second row shows the normalized spectrogram of the right M1 cortex collected chronically from a patient affected by ET and implanted with Activa PC + S. Two power bands centered at 15 and 25 Hz with 5-Hz bandwidth obtained with Fisher score feature selection were used as inputs to the linear discriminant analysis classifier embedded event detector (blue blocks indicate movement detection). The bottom row shows the output of the embedded event detector triggered closed-loop stimulation (stimulation range = 0 to 2 V, ramp-up/down = 2 V/s, frequency = 130 Hz, pulse width = 120 μs).

hoc testing identified a significant reduction in TEED with respect to DBS type ($t_9 = 12.89$, $P = 4.189 \times 10^{-7}$). Comparing CL-DBS TEED to the OL-DBS TEED, taking into consideration the reduction in stimulation parameters (such as pulse width) needed for paresthesia avoidance during CL-DBS (stimulation ramp-up), the mean energy saving improved to 67.93% (SD = 16.67%) within clinic testing [monthly percent energy usage (fig. S6A) and group energy saving (fig. S6B, left)] and 62.67% (SD = 14.26%) while at home (fig. S6B, right). For completeness, there is an estimated extra 10% in power consumption due to the internal event detector (Nexus-E) and sensing circuitry (*28*, *29*, *39*), compared to the OL-DBS condition. Nonetheless, one of the benefits of energy savings is the crucial increase in battery life, ultimately reducing battery replacement surgeries. Even considering that novel battery chemistries and recharging capabilities are being added to the new generation of neurostimulators, the systems will still benefit from a reduced power consumption due to CL-DBS, decreasing the number of needed recharges and decreasing the burden on the patient (*40*).

Longitudinal stability of CL- DBS (6 months)

A critical component of a closed-loop system is a chronically stable control feature. Our study showed the repeatability of a CL-DBS paradigm across 3 to 4 months. Table S2 shows that the CL-DBS algorithm required retraining only in one instance, for ET01 at month 6, because the change in therapeutic stimulation frequency as identified by a clinician (usage of 180-Hz stimulation) altered the feature space used previously (due to stimulation subharmonic artifacts). In addition, the maximum LFO decreases during contralateral movement initiation and termination [group power spectral density (PSD) average in fig. S7A and individual PSD LFO drop in fig. S7B] did not exhibit a statistically significant trend over time (mixed-model ANOVA with unnormalized PSD LFO bin, main effect of time: $F_{5,11} = 0.49540$, $P = 0.7736$). The drift of the LFO maximum decrease during contralateral movement was 1.85 dB/month (SD = 0.97 dB/month), which we considered being within an acceptable range, similar to a previous study that included subdural strips (*41*). In addition, we observed that the feature was not correlated ($R^2 = 0.0427$, $P = 0.4262$) to the impedance over the recording contacts (fig. S7C) considering the 12.35%/month (SD = 9.01%/month) drift in impedance over time (mixed-model ANOVA, main effect of time: $F_{5,11} = 7.8007$, $P = 0.0023$) (fig. S7D). However, impedance and power are likely to stabilize over time, as reported in previous studies with long-term cortical implants (*42*–*44*). In addition, the CL-DBS detector did not trigger stimulation during other nonmovement actions, such as speech. This is shown through a speech execution task with CL-DBS detector active, in which the patient switched between talking and rest periods without eliciting stimulation delivery (fig. S8A, single subject). The power deviations in the closed-loop feature bands during speech were not sufficient to elicit the delivery of full therapeutic stimulation (fig. S8B). This helped avoid undesirable stimulation-induced side effects.

Patient reporting for CL-DBS usage

No detectable difference between CL-DBS and OL-DBS settings (in tremor suppression performance) were reported by the patients. ET02 also self-reported benefit from CL-DBS related to the decreased incidence of DBS-induced speech impairment. ET03 preferred to use the CL-DBS, commenting that the algorithm was well tuned for his use, whereas ET01 expressed no preference. In addition, although subjects were advised to switch off CL-DBS while sleeping, between the consecutive daily visits at each month, frequently they did not disable CL-DBS. Nonetheless, they did not report any adverse effects or any trouble while sleeping (table S3). Because of device memory limitations, we were not able to record data while the patients were asleep. Hence, we report that the use of CL-DBS does not add unexpected adverse events during the time it was deployed (between consecutive daily visits at each month).

DISCUSSION

This study demonstrates the feasibility and implementation of closed-loop stimulation for patients affected by ET used in a fully embedded

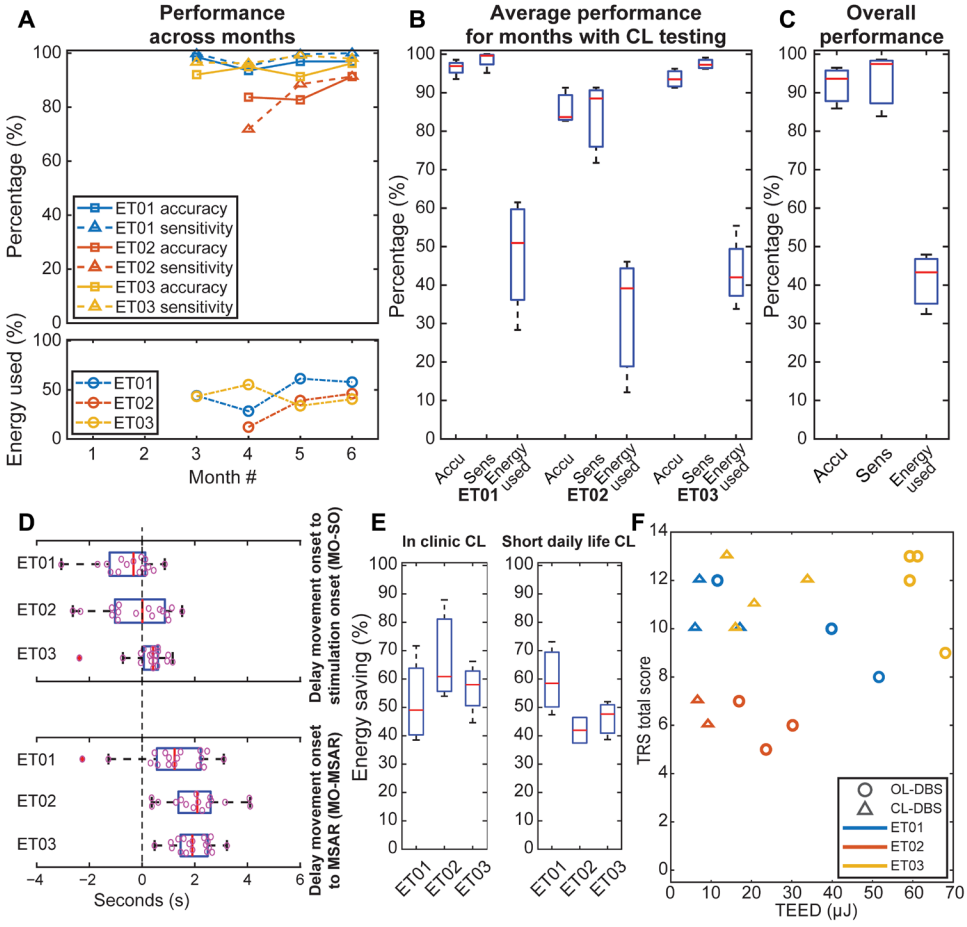

Fig. 6. Performances of CL-DBS at monthly visits in all the enrolled subjects using the fully embedded onboard PC + S algorithm. (**A**) Performances over the monthly clinical/research visit, such as accuracy and sensitivity of the CL-DBS classifier on top, and energy usage compared to energy usage (TEED) of continuous stimulation (with CL-DBS settings delivered as open-loop paradigm) at the bottom. (**B**) Average performances across months with CL-DBS during clinical/research visit. (**C**) Average performances of CL-DBS, including energy usage compared to energy usage (TEED) of continuous stimulation (with CL-DBS settings delivered as open-loop paradigm). (**D**) Characterization of the delays in the CL-DBS implementation (intervals MO-SO and MO-MSAR). (**E**) Energy saving with closed-loop stimulation compared to continuous stimulation (with CL-DBS settings delivered as open-loop paradigm) during clinical/research visit [as in (A) (bottom), (B), and (C)] and at short-term daily life usage. (**F**) TRS versus TEED scatterplot, showing a subject-based decrease in the overall CL-DBS TEED compared to OL-DBS while maintaining a comparable TRS. TEEDs are normalized to the duration of the task to avoid bias due to each task length.

system both in-clinic and at-home environments. The proposed paradigm for stimulation delivery used M1 as a driver for the DBS controller, achieving tremor suppression during movement in three patients. Consequently, it achieved integration with the patient behavior, a feature that is still lacking in currently commercially available DBS devices. Considering that the subset of the patient population enrolled in this study presented tremor mainly when moving, with the MO preceding the tremor onset, the movement biomarker was considered sufficient to target such pathological manifestation and facilitated DBS actuation in a timely manner before the manifestation of tremor. Tremor-specific features should be further explored; however, for our patient sample with intention tremor, movement-based features provided a reliable and tolerable control policy with rapid stimulation delivery that overcame stimulation artifact issues.

Our data, along with other recent studies (*45*–*50*), showed that it is possible to directly use the VIM to detect movement and tremor features. However, the stimulation would adversely affect recording quality, especially when delivering stimulation to contacts adjacent to the recording site, rendering the detection of the termination of movement/tremor impossible. In addition, other studies used external amplifiers connected to externalized electrodes or to single-unit recording setups with a more favorable signal-to-noise ratios, which have power consumption and form factors currently beyond what is feasible in the available implantable systems, considering that the DBS implants require considerable longevity to avoid battery replacement surgeries (*29*). Newer platforms are under development to address this shortcoming (*51*). Including a nontarget DBS area for the sensing (from M1) placed fewer constraints on the stimulation parameter space, avoiding the interdependence of stimulation and sensing contacts (bipolar sensing with symmetric contacts around a single contact used for monopolar stimulation). Nonetheless, our paradigm required the insertion of an additional subdural strip over the motor cortex, which had no previously known clinical benefit in an OL-DBS scenario and is not part of the usual standard of care. However, it required little to no variation to the standard DBS implantation surgery, using similar surgical constraints to the DBS lead targeting. The placement can be performed at the same time as the DBS lead implantation through the same burr hole, and it has currently not been associated with adverse outcomes when used in our long-term studies (*41*) and within other groups performing similar implants (*39*, *52*, *53*). Although other previous studies used a similar stimulation delivery approach based on cortical detection, they required the presence of an external controller (computer-in-the-loop with a telemetry wand) and lacked a longer-term evaluation of the paradigm during a realistic daily life scenario (in the clinic and at home) (*54*).

As onset of stimulation may commonly cause paresthesia in open-loop approaches, we had to optimize CL-DBS for tolerability. Although a slower ramp-up of stimulation amplitude improved tolerability, we also aimed to initiate therapeutic stimulation before tremor manifestation. Because movement preceded the tremor onset, our embedded classifier was able to initiate DBS with an optimized slope that could suppress tremor and avoid paresthesia. The CL-DBS users had a good response to the proposed stimulation paradigm. Tremor increased at the beginning of the movement, independent of the

timing of stimulation delivery (DBS OFF, OL-DBS, and CL-DBS). As shown in Fig. 4D, this is not bounded to the CL-DBS setup but is a problem also present in OL-DBS. Nonetheless, considering the shortness of the interval of interest [MO-MSAR, 1.72 s (SD = 1.15 s)], the modest decrease in tremor amplitude compared to DBS OFF seems sufficient to not create discomfort to the subject while executing a movement, as reported in previous OL-DBS studies (*3*, *24*). Analysis of the TEED during CL-DBS was shown to be lower compared to OL-DBS. The blinded clinical scores (TRS) and tremor amplitude showed equal effectiveness for both DBS settings (OL-DBS and CL-DBS).

Preliminary findings on other clinical benefits of CL-DBS seem to indicate that this stimulation paradigm can help address DBS-induced impairment, because it delivered DBS only when the patient presented tremor-related movement. The timing of DBS in response to patient symptoms is an important driver for the reduction of side effects. The reduction of DBS parameters (amplitude, pulse width, and frequency) can also contribute to the reduction of side effects, but it is only beneficial if it maintains the same therapeutic benefit, as shown in our data. In addition, because of the lack of unexpected adverse events during the deployment of this paradigm, including the cases where CL-DBS was left active during sleep, we conclude that CL-DBS appears to be safely implementable. Further out-of-clinic testing (daily life scenarios) will be pursued in the next phase of this study.

We observed that cortical placement was an important factor in our paradigm. Hence, we assumed that ET02 had the worst performance with an accuracy of 85.90% (SD = 4.71%) and sensitivity of 83.86% (SD = 10.57%) of the three subjects because of a less than optimal cortical placement, as only a single contact was above the precentral gyrus and consequently all bipolar combinations included non-M1 areas. The cause behind the suboptimal placement can be found in the surgical avoidance of conspicuous blood vessels.

Limitations in this study included restrictions for the classification algorithm, which was limited to the implementation of a simple linear classifier (see the "Embedded classification and debugging" section in Materials and Methods) with a single threshold control strategy, which, in the future, could be expanded in second-generation bidirectional neurostimulators with more flexibility (*55*). A wider set of features and advanced algorithms could increase the performance for the actuation of CL-DBS. Moreover, current device limitations did not allow reliable detection of broadband high gamma (BHG) activity from the power estimators used by the embedded detector. BHG activity modulates the most during contralateral movement and is more local (*56*–*59*). We expect that improved device noise floor would enable the use of BHG features for more reliable movement detection (*55*), leading to a more stable MO-SO interval across patients and avoiding to trigger stimulation during ipsilateral movement. However, we argue that being able to detect and stimulate for both ipsilateral and contralateral movement from a single location could be beneficial, because it requires only one side for cortical implantation, and previous studies have shown benefit from ipsilateral stimulation on tremor severity (*60*, *61*). Future studies should evaluate the performances of CL-DBS detection in a wider set of movements, such as walking, to ensure accuracy of stimulation delivery. Hence, considering the locality of BHG (*56*–*59*), detection based on BHG features could help address shortcomings of LFO-based detection, such as cross-site activation (feet motor areas). However, we showed that the current LFO-based detection was able to avoid spurious detection during speech, even considering the proximity of hand motor areas to face-related areas (*62*). Additional limitations of this study were the limited sample size (three patients), the focus on detection only during upper limb movements, and the lack of quantitative measures of side effects such as speech impairment. Larger longitudinal studies are needed to account for the quantification of efficacy and side effects, together with testing a wider set of movements in real-life scenarios, such as reaching for objects while walking. Improvements in neurostimulators are now in development, which could enable further detection capabilities and at-home testing scenarios (*55*). Furthermore, this study addresses the tremor manifestation during limb movement and does not address tremor manifesting in the head, neck, and voice.

Our goal for this study was to demonstrate the stability of a movement-based CL-DBS over time. This approach has considerably lower energy delivery, delivering stimulation only when needed, while maintaining clinical effectiveness in a range of movements (cup reaching, proximal and distal posture, water pouring, and writing). The proposed paradigm is a first step toward behaviorally modulated fully embedded DBS systems (*63*). This strategy requires an additional clinical step for the programming of the responsiveness of the controller. However, we note that the training sessions required little to no effort, because the system was using simple tasks. In summary, this work illustrates a comprehensive strategy for the training and deployment of CL-DBS therapies that are completely embedded within the patient's body, are responsive to real-time patient behavior, and integrate seamlessly with daily life activities.

MATERIALS AND METHODS

Study design

The aim of this study was to show the feasibility and implementation of a self-adjusting therapeutic DBS for patients affected by ET, based on motor behavior detection.

Neurological data were collected from M1 and VIM from the Activa PC + S neurostimulator over six monthly visits after surgery in three patients affected by ET. Blinded raters scored patients' clinical outcomes (TRS) in an in-subject crossover protocol (DBS OFF, OL-DBS, and CL-DBS). The patient was blinded to which setting was being tested during the clinical evaluation (TRS). No randomization was present in this study, because all patients were being tested in all three conditions (DBS OFF, OL-DBS, and CL-DBS). Subjects were enrolled in our study if they qualified within the inclusion and exclusion criteria as reported at Clinicaltrials.gov: NCT02649166. No patients were excluded after implantation of Activa PC + S. Enrollment inclusion and exclusion criteria are reported in the "Selection criteria" section in Supplementary Materials and Methods. Sample sizes were derived from patient availability and feasibility of enrollment at the University of Florida. Moreover, the study is sized appropriately for a feasibility pilot study, with neurotechnology being explored for the proposed application space. The subject numbers are consistent with published reports in the literature for DBS including recent examples from depression (*64*), obsessive compulsive disorder (*65*), and Tourette's syndrome (*66*). The sample size is also in line with regulatory expectations [U.S. Food and Drug Administration (FDA)] for pilot feasibility efforts. The first month was dedicated to integrating information from anatomical images and intraoperative recordings for assessing the best contacts for data acquisition. Initial testing revealed that bipolar stimulation of VIM

caused the least amount of stimulation artifact in the cortical channel (fig. S2).

Participants

We received FDA and University of Florida Institutional Review Board approval (ET Closed Loop DBS Study, ClinicalTrials.gov: NCT02649166) for a CL-DBS study to treat 10 patients with medically refractory ET using Medtronic Activa PC + S neurostimulators (*27*). To date, we enrolled three patients at the University of Florida Norman Fixel Institute for Neurological Diseases (table S1).

Experimental task design

The subjects performed five tasks: (i) Baseline, in which the subject was asked to remain still in a resting position, without contracting muscles to maintain any posture. (ii) Cued-go hand opening and closing, in which the subject was cued to open and close their left or right hand in a random order. When cued, the subject had to prepare to move with a specific hand (CUE, for 1.5 ± 0.5 s). Next, the subject was cued for how long to perform the movement (GO CUE, for 6.5 ± 0.5 s). Each moving phase was stopped by a rest cue, where the subject returned to the resting position used during the baseline task for 6.5 ± 1.5 s (Fig. 3A, top). (iii) Cued-go cup reaching, in which the subject was asked to reach a cup, bring it toward their mouth, and bring it back to the hand of the operator/researcher, in the original position. Only one hand was used at a time. The subject was cued to prepare to reach the cup with a specific hand (CUE, for 2 ± 1 s), requiring no actual movement during this phase, and then a second cue (GO CUE) indicated to initiate the movement (Fig. 3A, bottom). Between the GO CUE and the next CUE, there was an interval of 12 ± 2 s. In addition, the patient had to simulate the drinking action with the cup, by bringing it toward themselves, next to their mouth, and back to the original position to evoke tremor. (iv) Self-initiated cup reaching, in which the subject executed the previous task without being cued for which hand to use and when the movement had to start. The rest interval was also self-selected by the subject. (v) Postural tremor task [block = ~20 s; three times distal posture, three times proximal posture, randomized; interstimulus interval (ISI) = 20 s]. Tasks were executed with and without DBS. When cups were used, they were filled with water to evoke tremor. Local field potentials were acquired at 793.6 and 422 Hz in standalone mode (hardware lowpass at 100 Hz) with power channels disabled, unless a close-loop testing was in progress (with Nexus-E). EMG and inertia (accelerometer, gyroscope, and magnetometer) data were acquired at 1000 and 148.25 Hz, respectively (Trigno Wireless EMG, Delsys). The EMG/inertia sensors were placed on the patients' upper limbs (hand dorsum, flexor carpi ulnaris, and bicep on both arms) to detect MO/tremor. Video data were acquired at 24 Hz to capture behavioral activity. All the sources but the PC + S were aligned with a train of square pulses ("sync trigger") delivered to a dedicated shared channel, expanded from the setup used in previous work (*33*). The alignment of the neural data collected with Activa PC + S with EMG (and therefore the other sources) was achieved by delivering a short stimulation burst (~2 s) at 5 Hz. The stimulation termination could be detected both in the DBS lead and in the EMG positioned near the neck, where the DBS extension cable was passing. The alignment was executed at the beginning of each run execution. Once we had viable features for movement detection, at the third month, we proceeded to program and to optimize the CL-DBS implementation. In addition, we currently are seeking approval for letting the patients use the embedded CL-DBS system at home, between the monthly visits.

DBS programming, clinical evaluation, and short-term daily real-life usage

The patients underwent DBS programming as standard clinical care, optimizing the effectiveness of the stimulation to suppress the symptoms. The same clinical setting for open-loop stimulation was used as basis for closed-loop programming. Often, the closed-loop stimulation parameters had to be reduced to prevent paresthesia due to a fast SO, which was mild in intensity but could lead to discomfort. The Fahn-Tolosa-Marin TRS was used for clinical evaluation (*34*). The DBS OFF, OL-DBS, and CL-DBS effects on tremor and hand function were assessed at every follow-up visit. The neurologist and patient were blinded to avoid bias. Furthermore, CL-DBS energy saving was also evaluated during a typical daily real-life usage (labeled as short-term daily usage), in the time between two consecutive daily visits, from the afternoon to the morning of the next day. Because we could not directly measure the tremor outside the clinic, we could only estimate energy usage based on the detection, stimulation, and neural features logs. We also relied on the patient feedback to know whether the paradigm tested was effective in suppressing their tremor when at home (during the short-term daily usage).

Signal processing of neural signals and accelerometer data

All analyses were executed within the MATLAB 2018a environment (MathWorks) with custom scripts. Medtronic provided libraries to enable interfacing with the Activa PC + S neurostimulator.

As a first preprocessing step, the recorded channels (two bipolar configurations, one cortical and one thalamic) were inspected for artifacts and signal quality through visual inspection of the raw time series, the PSDs across tasks, and the spectrograms. An additional high-pass filter at 1 Hz was used to eliminate the time series drift and to reject low-frequency device noise. No channels were dropped from the subsequent analyses. PSDs and spectrograms were computed by using an autoregressive model (*67*, *68*) with a frequency resolution of 1 Hz.

Accelerometer data were analyzed for tremor amplitude quantification, by using the most distal sensors (hands). The tremor amplitude was computed by calculating the triaxial magnitude of the accelerometer amplitude profiles. The data were band-passed at the tremor frequency, using a Hilbert transform to obtain the amplitude envelope for each axis before point-by-point magnitude calculation. The tremor frequency was selected by looking at the frequency with a clear peak in power in the PSD in the presence of tremor symptoms.

Embedded classification and debugging

The onboard classifier of the Activa PC + S implanted neurostimulator was programmed based on a linear discriminant analysis (LDA) algorithm, the only available embedded classifier, which takes up to two power bands specified a priori as inputs. The system allows for the selection of the center frequency and bandwidth for the calculation of one power band (minimum bandwidth was 5 Hz). These power channels are based on analog power estimators sampled with 10-bit ADCs (analog to digital converters), which are separate from the ADC used to sample the raw trace (*27*, *29*, *51*). Hence, offline training based only on spectral estimation of the power

channels from the time series signal yielded unreliable results when used to directly obtain the weights for the embedded LDA algorithm. In addition, the stimulation affected the power channels when active, leading to a variety of effects such as saturation (with unrecoverable neuromarkers), major artifacts (with unrecoverable neuromarkers, as in fig. S1), and minor artifacts (with recoverable neuromarkers, as in Fig. 5 and figs. S2 and S3). Many combinations of power settings and DBS settings could lead to power modulation (power increase) when stimulation was delivered, increasing the risk of going over the detection threshold and possibly causing a continuous toggling between stim-on/stim-off state (fig. S9). The Medtronic Activa PC + S device is enabled for onboard logging of additional information and internal states together with the neural activity, such as the detection status (detection True/False). To verify accurate stimulation delivery, we filtered the cortical activity with a bandpass filter centered around the stimulation frequency (fig. S10). We chose to compute the estimate of the delivered stimulation using the detection state (internal LDA) and the neurostimulator parameters (amplitude, ramp-up time, ramp-down time, detection onset delay, and detection termination delay), leading to a cleaner trace. Its reliability was tested by comparing the two estimates (fig. S10).

Risk and mitigations

The deployment of the system in a complex scenario, taking into consideration a large variety of potential issues and pitfalls, required the presence of safety mechanisms for the protection of the patient. A possible case would be when there could be a failure of the sensing stage of the implanted neurostimulator. Other case scenarios were stimulation artifact and edge cases that cause stimulation toggling (fig. S9), which could be possibly encountered due to progressive drift of the acquisition stage (power estimates) over time. To that end, a fallback "safe" mode (*30*) was provided to the subject, which was quickly available by using the provided patient programmer. In our cohort, we did not encounter any device failures. The role of this mode was to quickly provide a clinically approved stimulation state to deliver a therapeutic DBS with no interruption to the patient benefit.

Statistical analyses

MATLAB statistical package was used (R2018a). Data were tested for normal (Gaussian) distribution using Shapiro-Wilk normality test. All correlation are Pearson, and all P values are two-tailed, except in the TOST procedure (*69*, *70*). A P value of <0.05 was considered statistically significant (P value is specified). In addition, each statistic technique used is mentioned individually within Results. Repeated measures were tested with a mixed-model ANOVA. Specifically, we used the subsequent models for each of these results: TRS deviation from DBS OFF for CL-DBS and OL-DBS, mixed-model ANOVA with patient as random effect "TRS_score~DBS_type+(1|pat_id)"; amplitude change from DBS OFF for CL-DBS and OL-DBS, mixed-model ANOVA with patient as random effect "acceleration_amplitude~DBS_type+(1|pat_id)"; the same model was used for the MO-MSAR and MSAR-MT acceleration amplitudes; energy saving evaluation based on TEED comparisons across different stimulation settings (DBS OFF, OL-DBS, and CL-DBS), mixed-model ANOVA with patient as random effect "TEED~TRS_score*DBS_type+(1|pat_id)"; PSD stability over time was evaluated with a mixed-model ANOVA with patient as random effect "power_LFO~months+(1|pat_id)"; impedance stability over time was evaluated with a mixed-model ANOVA with patient as random effect "impedance~month+(1|pat_id)".

SUPPLEMENTARY MATERIALS

stm.sciencemag.org/cgi/content/full/12/572/eaay7680/DC1

Materials and Methods

Fig. S1. Artifacts from stimulation impaired data collection from VIM contacts.

Fig. S2. Artifacts from stimulation did not impair movement detection performances from cortical contacts.

Fig. S3. Implementation of CL-DBS in a patient affected by ET showing spectral leakage of the stimulation artifact.

Fig. S4. Performances of the embedded detector over the monthly clinical/research visit in all the enrolled subjects.

Fig. S5. TRS improvements versus TEED savings in percent.

Fig. S6. Energy performance of CL-DBS at monthly visits in all the enrolled subjects compared to OL-DBS energy consumption (TEED).

Fig. S7. PSD and impedance over a 6-month period.

Fig. S8. Performance of CL-DBS in patients affected by ET during speech execution.

Fig. S9. Example of a non-optimized embedded closed-loop stimulation paradigm.

Fig. S10. Stimulation delivery estimated by two different methodologies.

Table S1. Subject demographics for the study.

Table S2. DBS and closed-loop settings at each month for each patient during TRS clinical evaluation.

Table S3. DBS-related side effects and preference reported.

Movie S1. Comparison between DBS OFF, CL-DBS (fully embedded implementation), and OL-DBS in ET01 during a volitional movement task.

Movie S2. Comparison between DBS OFF, CL-DBS (fully embedded implementation), and OL-DBS in ET02 during a cued-go cup reaching task.

Movie S3. Comparison between DBS OFF, CL-DBS (fully embedded implementation), and OL-DBS in ET03 during a volitional cup reaching task.

Data file S1. Data for Figs. 2 to 6 and figs. S3, S4, and S6 (provided as separate Excel file).

Data file S2. Data for figs. S1, S2, S5, and S7 to S10 (provided as separate Excel file).

References (*71*–*80*)

View/request a protocol for this paper from *Bio-protocol*.

REFERENCES AND NOTES

1. J. A. Semrau, T. M. Herter, Z. H. Kiss, S. P. Dukelow, Disruption in proprioception from long-term thalamic deep brain stimulation: A pilot study. *Front. Hum. Neurosci.* **9**, 244 (2015).
2. D. Mücke, J. Becker, M. T. Barbe, I. Meister, L. Liebhart, T. B. Roettger, T. Dembek, L. Timmermann, M. Grice, The effect of deep brain stimulation on the speech motor system. *J. Speech Lang. Hear. Res.* **57**, 1206–1218 (2014).
3. T. A. Zesiewicz, J. D. Shaw, K. G. Allison, J. S. Staffetti, M. S. Okun, K. L. Sullivan, Update on treatment of essential tremor. *Curr. Treat. Options Neurol.* **15**, 410–423 (2013).
4. D. Mücke, A. Hermes, T. B. Roettger, J. Becker, H. Niemann, T. A. Dembek, L. Timmermann, V. Visser-Vandewalle, G. R. Fink, M. Grice, M. T. Barbe, P. Gonzalez-Alegre, The effects of thalamic deep brain stimulation on speech dynamics in patients with essential tremor: An articulographic study. *PLOS ONE* **13**, e0191359 (2018).
5. K. T. Mitchell, P. Larson, P. A. Starr, M. S. Okun, R. E. Wharen Jr., R. J. Uitti, B. L. Guthrie, D. Peichel, R. Pahwa, H. C. Walker, K. Foote, F. J. Marshall, J. Jankovic, R. Simpson, F. Phibbs, J. S. Neimat, R. M. Stewart, K. Dashtipour, J. L. Ostrem, Benefits and risks of unilateral and bilateral ventral intermediate nucleus deep brain stimulation for axial essential tremor symptoms. *Parkinsonism Relat. Disord.* **60**, 126–132 (2019).
6. J. G. Pilitsis, L. V. Metman, J. R. Toleikis, L. E. Hughes, S. B. Sani, R. A. E. Bakay, Factors involved in long-term efficacy of deep brain stimulation of the thalamus for essential tremor. *J. Neurosurg. Pediatr.* **109**, 640–646 (2008).
7. C. G. Favilla, D. Ullman, A. Wagle Shukla, K. D. Foote, C. E. Jacobson, M. S. Okun, Worsening essential tremor following deep brain stimulation: Disease progression versus tolerance. *Brain* **135**, 1455–1462 (2012).
8. M. J. Birdno, A. M. Kuncel, A. D. Dorval, D. A. Turner, R. E. Gross, W. M. Grill, Stimulus features underlying reduced tremor suppression with temporally patterned deep brain stimulation. *J. Neurophysiol.* **107**, 364–383 (2012).
9. E. D. Louis, R. Ottman, How many people in the USA have essential tremor? Deriving a population estimate based on epidemiological data. *Tremor Other Hyperkinet. Mov. (N. Y.)* **4**, 259 (2014).
10. E. D. Louis, J. J. Ferreira, How common is the most common adult movement disorder? Update on the worldwide prevalence of essential tremor. *Mov. Disord.* **25**, 534–541 (2010).
11. E. D. Louis, L. Barnes, S. M. Albert, L. Cote, F. R. Schneier, S. L. Pulman, Q. Yu, Correlates of functional disability in essential tremor. *Mov. Disord.* **16**, 914–920 (2001).

12. S. P. Woods, J. C. Scott, J. A. Fields, A. Poquette, A. I. Tröster, Executive dysfunction and neuropsychiatric symptoms predict lower health status in essential tremor. *Cogn. Behav. Neurol.* **21**, 28–33 (2008).
13. D. Lorenz, D. Schwieger, H. Moises, G. Deuschl, Quality of life and personality in essential tremor patients. *Mov. Disord.* **21**, 1114–1118 (2006).
14. F. R. Schneier, L. F. Barnes, S. M. Albert, E. D. Louis, Characteristics of social phobia among persons with essential tremor. *J. Clin. Psychiatry* **62**, 367–372 (2001).
15. K. P. Bhatia, P. Bain, N. Bajaj, R. J. Elble, M. Hallett, E. D. Louis, J. Raethjen, M. Stamelou, C. M. Testa, G. Deuschl, Consensus statement on the classification of tremors. From the task force on tremor of the International Parkinson and Movement Disorder Society. *Mov. Disord.* **33**, 75–87 (2018).
16. G. Deuschl, R. Wenzelburger, K. Löffler, J. Raethjen, H. Stolze, Essential tremor and cerebellar dysfunction clinical and kinematic analysis of intention tremor. *Brain* **123**, 1568–1580 (2000).
17. P. Feys, W. Helsen, A. Lavrysen, B. Nuttin, P. Ketelaer, Intention tremor during manual aiming: A study of eye and hand movements. *Mult. Scler.* **9**, 44–54 (2003).
18. W. J. Elias, B. B. Shah, Tremor. *JAMA* **311**, 948–954 (2014).
19. E. D. Louis, E. Rios, C. Henchcliffe, How are we doing with the treatment of essential tremor (ET)?: Persistence of patients with ET on medication: Data from 528 patients in three settings. *Eur. J. Neurol.* **17**, 882–884 (2010).
20. M. F. Brin, K. E. Lyons, J. Doucette, C. H. Adler, J. N. Caviness, C. L. Comella, R. M. Dubinsky, J. H. Friedman, B. V. Manyam, J. Y. Matsumoto, S. L. Pullman, A. H. Rajput, K. D. Sethi, C. Tanner, W. C. Koller, A randomized, double masked, controlled trial of botulinum toxin type A in essential hand tremor. *Neurology* **56**, 1523–1528 (2001).
21. V. Castrillo-Fraile, E. C. Peña, J. M. T. Gabriel Y Galán, P. D. Delgado-López, C. Collazo, E. Cubo, Tremor control devices for essential tremor: A systematic literature review. *Tremor Other Hyperkinet. Mov. (N. Y.)* **9**, (2019).
22. J. Á. Gallego, J. Ibanez, J. L. Dideriksen, J. I. Serrano, M. D. Del Castillo, D. Farina, E. Rocon, A multimodal human-robot interface to drive a neuroprosthesis for tremor management. *IEEE Trans. Syst. Man Cybern. Part C Appl. Rev.* **42**, 1159–1168 (2012).
23. F. B. Nahab, E. Peckham, M. Hallett, Essential tremor, deceptively simple. *Pract. Neurol.* **7**, 222–233 (2007).
24. A. Chopra, B. T. Klassen, M. Stead, Current clinical application of deep-brain stimulation for essential tremor. *Neuropsychiatr. Dis. Treat.* **9**, 1859–1865 (2013).
25. J. A. Brodkey, R. R. Tasker, C. Hamani, M. P. McAndrews, J. O. Dostrovsky, A. M. Lozano, Tremor cells in the human thalamus: Differences among neurological disorders. *J. Neurosurg.* **101**, 43–47 (2004).
26. P. Khanna, S. Stanslaski, Y. Xiao, T. Ahrens, D. Bourget, N. Swann, P. Starr, J. M. Carmena, T. Denison, Enabling closed-loop neurostimulation research with downloadable firmware upgrades, in *Proceedings of the IEEE Biomedical Circuits and Systems Conference: Engineering for Healthy Minds and Able Bodies (BioCAS 2015)* (Institute of Electrical and Electronics Engineers Inc., 2015), pp. 1–6.
27. S. Stanslaski, P. Afshar, P. Cong, J. Giftakis, P. Stypulkowski, D. Carlson, D. Linde, D. Ullestad, A.-T. Avestruz, T. Denison, Design and validation of a fully implantable, chronic, closed-loop neuromodulation device with concurrent sensing and stimulation. *IEEE Trans. Neural Syst. Rehabil. Eng.* **20**, 410–421 (2012).
28. P. Afshar, A. Khambhati, S. Stanslaski, D. Carlson, R. Jensen, D. Linde, S. Dani, M. Lazarewicz, P. Cong, J. Giftakis, P. Stypulkowski, T. Denison, A translational platform for prototyping closed-loop neuromodulation systems. *Front. Neural Circuits* **6**, 117 (2012).
29. A.-T. Avestruz, W. Santa, D. Carlson, R. Jensen, S. Stanslaski, A. Helfenstine, T. Denison, A 5 μW/channel spectral analysis IC for chronic bidirectional brain-machine interfaces. *IEEE J. Solid State Circuits* **43**, 3006–3024 (2008).
30. A. Gunduz, E. Opri, R. Gilron, V. Kremen, G. Worrell, P. Starr, K. Leyde, T. Denison, Adding wisdom to 'smart' bioelectronic systems: A design framework for physiologic control including practical examples. *Bioelectron. Med.* **2**, 29–41 (2019).
31. C. R. Butson, S. E. Cooper, J. M. Henderson, C. C. McIntyre, Patient-specific analysis of the volume of tissue activated during deep brain stimulation. *Neuroimage* **34**, 661–670 (2007).
32. C.-u. Choe, U. Hidding, M. Schaper, A. Gulberti, J. Köppen, C. Buhmann, C. Gerloff, C. K. E. Moll, W. Hamel, M. Pötter-Nerger, Thalamic short pulse stimulation diminishes adverse effects in essential tremor patients. *Neurology* **91**, e704–e713 (2018).
33. E. Opri, S. Cernera, M. S. Okun, K. D. Foote, A. Gunduz, The functional role of thalamocortical coupling in the human motor network. *J. Neurosci.* **39**, 8124–8134 (2019).
34. S. Fahn, E. Tolosa, C. Marin, Clinical rating scale for tremor, in *Parkinson's Disease and Movement Disorders*, J. Jankovic, E. Tolosa, Eds. (Williams and Wilkins, 1993), pp. 271–280.
35. M. A. Stacy, R. J. Elble, W. G. Ondo, S.-C. Wu, J. Hulihan, Assessment of interrater and intrarater reliability of the Fahn-Tolosa-Marin Tremor Rating Scale in essential tremor. *Mov. Disord.* **22**, 833–838 (2007).
36. H. Cagnan, J.-S. Brittain, S. Little, T. Foltynie, P. Limousin, L. Zrinzo, M. Hariz, C. Joint, J. Fitzgerald, A. L. Green, T. Aziz, P. Brown, Phase dependent modulation of tremor amplitude in essential tremor through thalamic stimulation. *Brain* **136**, 3062–3075 (2013).
37. H. Cagnan, D. Pedrosa, S. Little, A. Pogosyan, B. Cheeran, T. Aziz, A. Green, J. Fitzgerald, T. Foltynie, P. Limousin, L. Zrinzo, M. Hariz, K. J. Friston, T. Denison, P. Brown, Stimulating at the right time: Phase-specific deep brain stimulation. *Brain* **140**, 132–145 (2016).
38. A. M. Koss, R. L. Alterman, M. Tagliati, J. L. Shils, Calculating total electrical energy delivered by deep brain stimulation systems. *Ann. Neurol.* **58**, 168 (2005).
39. N. C. Swann, C. de Hemptinne, M. C. Thompson, S. Miocinovic, A. M. Miller, R. Gilron, J. L. Ostrem, H. J. Chizeck, P. A. Starr, Adaptive deep brain stimulation for Parkinson's disease using motor cortex sensing. *J. Neural Eng.* **15**, 046006 (2018).
40. T. Khaleeq, H. Hasegawa, M. Samuel, K. Ashkan, Fixed-life or rechargeable battery for deep brain stimulation: Which do patients prefer? *Neuromodulation* **22**, 489–492 (2018).
41. J. B. Shute, M. S. Okun, E. Opri, R. Molina, P. J. Rossi, D. Martinez-Ramirez, K. D. Foote, A. Gunduz, Thalamocortical network activity enables chronic tic detection in humans with Tourette syndrome. *NeuroImage Clin.* **12**, 165–172 (2016).
42. K. A. Sillay, P. Rutecki, K. Cicora, G. Worrell, J. Drazkowski, J. J. Shih, A. D. Sharan, M. J. Morrell, J. Williams, B. Wingeier, Long-term measurement of impedance in chronically implanted depth and subdural electrodes during responsive neurostimulation in humans. *Brain Stimul.* **6**, 718–726 (2013).
43. K. A. Sillay, S. Ondoma, B. Wingeier, D. Schomberg, P. Sharma, R. Kumar, G. S. Miranpuri, J. Williams, Long-term surface electrode impedance recordings associated with gliosis for a closed-loop neurostimulation device. *Ann. Neurosci.* **25**, 289–298 (2018).
44. F. T. Sun, S. Arcot Desai, T. K. Tcheng, M. J. Morrell, Changes in the electrocorticogram after implantation of intracranial electrodes in humans: The implant effect. *Clin. Neurophysiol.* **129**, 676–686 (2018).
45. H. Tan, J. Debarros, S. He, A. Pogosyan, T. Z. Aziz, Y. Huang, S. Wang, L. Timmermann, V. Visser-Vandewalle, D. J. Pedrosa, A. L. Green, P. Brown, Decoding voluntary movements and postural tremor based on thalamic LFPs as a basis for closed-loop stimulation for essential tremor. *Brain Stimul.* **12**, 858–867 (2019).
46. D. J. Pedrosa, P. Brown, H. Cagnan, V. Visser-Vandewalle, J. Wirths, L. Timmermann, J.-S. Brittain, A functional micro-electrode mapping of ventral thalamus in essential tremor. *Brain* **141**, 2644–2654 (2018).
47. S. E. Hua, F. A. Lenz, Posture-related oscillations in human cerebellar thalamus in essential tremor are enabled by voluntary motor circuits. *J. Neurophysiol.* **93**, 117–127 (2005).
48. A. Kane, W. D. Hutchison, M. Hodaie, A. M. Lozano, J. O. Dostrovsky, Enhanced synchronization of thalamic theta band local field potentials in patients with essential tremor. *Exp. Neurol.* **217**, 171–176 (2009).
49. C. Brücke, A. Bock, J. Huebl, J. K. Krauss, T. Schönecker, G.-H. Schneider, P. Brown, A. A. Kühn, Thalamic gamma oscillations correlate with reaction time in a Go/noGo task in patients with essential tremor. *Neuroimage* **75**, 36–45 (2013).
50. S. Little, A. Pogosyan, S. Neal, B. Zavala, L. Zrinzo, M. Hariz, T. Foltynie, P. Limousin, K. Ashkan, J. FitzGerald, A. L. Green, T. Z. Aziz, P. Brown, Adaptive deep brain stimulation in advanced Parkinson disease. *Ann. Neurol.* **74**, 449–457 (2013).
51. S. Stanslaski, J. Herron, T. Chouinard, D. Bourget, B. Isaacson, V. Kremen, E. Opri, W. Drew, B. H. Brinkmann, A. Gunduz, T. Adamski, G. A. Worrell, T. Denison, A chronically-implanted neural coprocessor for exploring treatments for neurological disorders. *IEEE Trans. Biomed. Circuits Syst.* **12**, 1230–1245 (2018).
52. N. C. Swann, C. de Hemptinne, S. Miocinovic, S. Qasim, J. L. Ostrem, N. B. Galifianakis, M. San Luciano, S. S. Wang, N. Ziman, R. Taylor, P. A. Starr, Chronic multisite brain recordings from a totally implantable bidirectional neural interface: Experience in 5 patients with Parkinson's disease. *J. Neurosurg.* **128**, 605–616 (2018).
53. F. Panov, E. Levin, C. de Hemptinne, N. C. Swann, S. Qasim, S. Miocinovic, J. L. Ostrem, P. A. Starr, Intraoperative electrocorticography for physiological research in movement disorders: Principles and experience in 200 cases. *J. Neurosurg.* **126**, 122–131 (2017).
54. B. Houston, M. Thompson, A. Ko, H. Chizeck, A machine-learning approach to volitional control of a closed-loop deep brain stimulation system. *J. Neural Eng.* **16**, 016004 (2019).
55. S. Stanslaski, J. Herron, T. Chouinard, D. Bourget, B. Isaacson, V. Kremen, E. Opri, W. Drew, B. H. Brinkmann, A. Gunduz, T. Adamski, G. A. Worrell, T. Denison, A chronically implantable neural coprocessor for investigating the treatment of neurological disorders. *IEEE Trans. Biomed. Circuits Syst.* **12**, 1230–1245 (2018).
56. K. J. Miller, S. Zanos, E. E. Fetz, M. den Nijs, J. G. Ojemann, Decoupling the cortical power spectrum reveals real-time representation of individual finger movements in humans. *J. Neurosci.* **29**, 3132–3137 (2009).
57. K. J. Miller, E. C. Leuthardt, G. Schalk, R. P. N. Rao, N. R. Anderson, D. W. Moran, J. W. Miller, J. G. Ojemann, Spectral changes in cortical surface potentials during motor movement. *J. Neurosci.* **27**, 2424–2432 (2007).
58. K. J. Miller, G. Schalk, E. E. Fetz, M. den Nijs, J. G. Ojemann, R. P. N. Rao, Cortical activity during motor execution, motor imagery, and imagery-based online feedback. *Proc. Natl. Acad. Sci. U.S.A.* **107**, 4430–4435 (2010).
59. T. Jiang, N. F. Ince, T. Jiang, T. Wang, S. Mei, Y. Li, X. Wang, Z. Sha, Local spatial correlation analysis of hand flexion/extension using intraoperative high-density ECoG, in

Proceedings of 37th Annual International Conference of the IEEE Engineering in Medicine and Biology Society (EMBS 2015) (IEEE, 2015), pp. 6190–6193.
60. W. Ondo, K. Dat Vuong, M. Almaguer, J. Jankovic, R. K. Simpson, Thalamic deep brain stimulation: Effects on the nontarget limbs. *Mov. Disord.* **16**, 1137–1142 (2001).
61. Z. Peng-Chen, T. Morishita, D. Vaillancourt, C. Favilla, K. D. Foote, M. S. Okun, A. Wagle Shukla, Unilateral thalamic deep brain stimulation in essential tremor demonstrates long-term ipsilateral effects. *Park. Relat. Disord.* **19**, 1113–1117 (2013).
62. J. Roland, P. Brunner, J. Johnston, G. Schalk, E. C. Leuthardt, Passive real-time identification of speech and motor cortex during an awake craniotomy. *Epilepsy Behav.* **18**, 123–128 (2010).
63. W.-J. Neumann, R. S. Turner, B. Blankertz, T. Mitchell, A. A. Kühn, R. M. Richardson, Toward electrophysiology-based intelligent adaptive deep brain stimulation for movement disorders. *Neurotherapeutics* **16**, 105–118 (2019).
64. C. S. Kubu, T. Brelje, M. A. Butters, T. Deckersbach, P. Malloy, P. Moberg, A. I. Tröster, E. Williamson, G. H. Baltuch, M. T. Bhati, L. L. Carpenter, D. D. Dougherty, R. H. Howland, A. R. Rezai, D. A. Malone Jr., Cognitive outcome after ventral capsule/ventral striatum stimulation for treatment-resistant major depression. *J. Neurol. Neurosurg. Psychiatry* **88**, 262–265 (2017).
65. L. Islam, A. Franzini, G. Messina, S. Scarone, O. Gambini, Deep brain stimulation of the nucleus accumbens and bed nucleus of stria terminalis for obsessive-compulsive disorder: A case series. *World Neurosurg.* **83**, 657–663 (2015).
66. L. Ackermans, A. Duits, C. van der Linden, M. Tijssen, K. Schruers, Y. Temel, M. Kleijer, P. Nederveen, R. Bruggeman, S. Tromp, V. van Kranen-Mastenbroek, H. Kingma, D. Cath, V. Visser-Vandewalle, Double-blind clinical trial of thalamic stimulation in patients with Tourette syndrome. *Brain* **134**, 832–844 (2011).
67. G. Schalk, D. J. McFarland, T. Hinterberger, N. Birbaumer, J. R. Wolpaw, BCI2000: A general-purpose brain-computer interface (BCI) system. *IEEE Trans. Biomed. Eng.* **51**, 1034–1043 (2004).
68. P. Stoica, R. L. Moses, *Spectral Analysis of Signals* (Pearson/Prentice Hall, 2005).
69. E. M. Rose, T. Mathew, D. A. Coss, B. Lohr, K. E. Omland, A new statistical method to test equivalence: An application in male and female eastern bluebird song. *Anim. Behav.* **145**, 77–85 (2018).
70. U. Meier, Nonparametric equivalence testing with respect to the median difference. *Pharm. Stat.* **9**, 142–150 (2009).
71. A. Sudhyadhom, M. S. Okun, K. D. Foote, M. Rahman, F. J. Bova, A three-dimensional deformable brain atlas for DBS targeting. I. Methodology for atlas creation and artifact reduction. *Open Neuroimag. J.* **6**, 92–98 (2012).
72. T. A. Yousry, U. D. Schmid, H. Alkadhi, D. Schmidt, A. Peraud, A. Buettner, P. Winkler, Localization of the motor hand area to a knob on the precentral gyrus. A new landmark. *Brain* **120**, 141–157 (1997).
73. C. Cedzich, M. Taniguchi, S. Schäfer, J. Schramm, Somatosensory evoked potential phase reversal and direct motor cortex stimulation during surgery in and around the central region. *Neurosurgery* **38**, 962–970 (1996).
74. S. A. Sheth, C. A. Eckhardt, B. P. Walcott, E. N. Eskandar, M. V. Simon, Factors affecting successful localization of the central sulcus using the somatosensory evoked potential phase reversal technique. *Neurosurgery* **72**, 828–834 (2013).
75. N. Maling, J. Shute, P. Rossi, C. de Hemptinne, J. Sanchez, B. Kretzman, A. Shukla, K. Foote, M. S. Okun, A. Gunduz, in Neuroscience Annual Meeting 2014, Washington, DC, 15 to 19 November 2014.
76. N. J. Hill, D. Gupta, P. Brunner, A. Gunduz, M. A. Adamo, A. Ritaccio, G. Schalk, Recording human electrocorticographic (ECoG) signals for neuroscientific research and real-time functional cortical mapping. *J. Vis. Exp.* , e3993 (2012).
77. B. B. Avants, N. J. Tustison, G. Song, P. A. Cook, A. Klein, J. C. Gee, A reproducible evaluation of ANTs similarity metric performance in brain image registration. *Neuroimage* **54**, 2033–2044 (2011).
78. B. B. Avants, C. L. Epstein, M. Grossman, J. C. Gee, Symmetric diffeomorphic image registration with cross-correlation: Evaluating automated labeling of elderly and neurodegenerative brain. *Med. Image Anal.* **12**, 26–41 (2008).
79. G. Schalk, E. C. Leuthardt, Brain-computer interfaces using electrocorticographic signals. *IEEE Rev. Biomed. Eng.* **4**, 140–154 (2011).
80. C. C. Aggarwal, *Data Classification: Algorithms and Applications* (Chapman and Hall, ed. 1, 2014).

Acknowledgments: We thank the patients for their availability and help in this study. We also thank K. Rizer for his administrative support. **Funding:** This work was supported by the NIH BRAIN Initiative through NINDS grant UH3NS095553 to A.G. and K.D.F. **Author contributions:** Conceptualization: E.O., T.D., A.G., and K.D.F.; data curation: E.O., L.A., and R.S.E.; formal analysis: E.O.; funding acquisition: A.G. and K.D.F.; investigation: E.O., S.C., R.M., and K.D.F.; methodology: E.O.; project administration: E.O. and A.G.; resources: A.G., T.D., M.S.O., and K.D.F.; software: E.O.; supervision: A.G. and M.S.O.; visualization: E.O., R.S.E., and J.N.C.; writing (original draft): E.O. and A.G.; writing (review and editing): A.G., S.C., T.D., M.S.O., and K.D.F. **Competing interests:** L.A. has provided educational consulting and participated in advisory boards, therefore receiving honoraria for such activities, for Medtronic and Boston Scientific. T.D. is a paid consultant for Synchron, CorTec Neurotechnology, and Inspire Sleep Therapy. His research is funded by the MRC (UK), DARPA, the Royal Academy of Engineering, and multiple foundation sources. Implantable devices for T.D.'s DBS-related research have been provided by Medtronic and Bioinduction. (Medtronic has provided implantable devices and some technical support for the current study.) He was a vice president of Research and Technology at Medtronic through August 2018. He has multiple patents in the area of brain-machine interfacing and DBS (9,248,288 and 8,380,314: Patient-directed therapy control; 8,554,325: Therapy control based on a patient movement state), all licensed to Medtronic, but receives no royalty payments. M.S.O. serves as a consultant for the Parkinson's Foundation and has received research grants from the NIH, the Parkinson's Foundation, the Michael J. Fox Foundation, the Parkinson Alliance, the Smallwood Foundation, the Bachmann-Strauss Foundation, the Tourette Syndrome Association, and the UF Foundation. M.S.O.'s DBS research is supported by R01 NR014852 and R01NS096008. M.S.O. has received royalties for publications with Demos, Manson, Amazon, Smashwords, Books4Patients, Perseus, Robert Rose, Oxford, and Cambridge (movement disorders books). M.S.O. is an associate editor for New England Journal of Medicine Journal Watch Neurology. M.S.O. has participated in CME and educational activities on movement disorders sponsored by the Academy for Healthcare Learning, PeerView, Prime, QuantiaMD, WebMD/Medscape, Medicus, MedNet, Einstein, Henry Stewart, American Academy of Neurology, Movement Disorders Society, and Vanderbilt University. The institution, and not M.S.O., receives grants from Medtronic, AbbVie, Abbott, and Allergan, and the principal investigator has no financial interest in these grants. M.S.O. has participated as a site principal investigator and/or coinvestigator for several NIH-, foundation-, and industry-sponsored trials over the years but has not received honoraria. Research projects at the University of Florida receive device and drug donations. K.D.F. has received occasional consulting fees from Medtronic and Boston Scientific. His research is primarily funded by the NIH and multiple foundation sources. Implantable devices for K.D.F.'s DBS-related research have been provided by Medtronic and NeuroPace. (Medtronic has provided implantable devices and some technical support for the current study.) K.D.F. has participated as a site implanting surgeon in multicenter DBS-related research studies sponsored by Abbott/St. Jude, Boston Scientific, and Functional Neuromodulation. The University of Florida receives partial funding for K.D.F.'s functional neurosurgery fellowship from Medtronic. **Data and materials availability:** All data associated with this study are present in the paper or the Supplementary Materials.

Submitted 17 July 2019
Resubmitted 14 January 2020
Accepted 25 August 2020
Published 2 December 2020
10.1126/scitranslmed.aay7680

Citation: E. Opri, S. Cernera, R. Molina, R. S. Eisinger, J. N. Cagle, L. Almeida, T. Denison, M. S. Okun, K. D. Foote, A. Gunduz, Chronic embedded cortico-thalamic closed-loop deep brain stimulation for the treatment of essential tremor. *Sci. Transl. Med.* **12**, eaay7680 (2020).